université angers FACULTÉ DE MÉDECINE

GEROM Groupe d'Etudes "Remodelage Osseux et bioMatériaux"
LHEA : Laboratoire d'Histologie – Embryologie

Short memo on texture analysis of bone radiographs

MAJ Dc 2014december
D. CHAPPARD

Rationale

Plain X-ray films are the most commonly used examinations in clinical practice for the diagnosis and surveillance of osteoporotic patients. A bone radiograph is a 2D projection of the 3D trabecular network, and several groups have considered that texture analysis of such images can provide valuable analysis of the trabecular architecture [1-7]. Trabecular microarchitecture is recognized as an important component of bone quality [8]. On an X-ray image, trabecular bone appears as « a texture » and the relationships with the 3-D original object, although intuitively dependent, are unknown. In some cases, the texture of the trabecular bone within the vertebral body may be an indicator of the etiology (e.g., the increased appearance of vertical trabeculae in corticosteroid osteoporosis). Texture is usually defined as « a global pattern arising from the repetition, either deterministically or randomly, of local sub-patterns ». Sub patterns are sometimes referred to as primitive elements in the image analysis literature (e.g., a tile is a primitive in a mosaic). Texture analysis of plain radiographs could represent an interesting clinical tool to describe bone architecture in pathological conditions and the method can be applied to alveolar bone.

Different algorithms have been proposed to measured bone on X-ray films. Our laboratory has described and applied a number of them that are summarized here:

On plain X-ray images obtained on calcaneus or radius, a 512 x 512 square is trimmed 2cm under the top of the iliac crest. This image is then used for texture

analysis after inversion (i.e., bone trabeculae in white) using the following techniques:

a) Skeletonization

Images are binarized by using an automatic threshold based on the histogram frequency distribution of grey levels [9].The threshold is chosen to be the peak of the image histogram (indicating the grey value of maximum occurrence). Pixels below the threshold are black-painted and considered to belong to marrow spaces. White pixels above the threshold are white painted and constituted the trabecular counterpart. The fractional surface area of white pixels is computed and represented the AREA parameter. Other morphologic parameters similar to those defined by Geraets et al., are used after skeletonization of the white set by thinning and pruning algorithms [5].

- BOUND is the total number of white pixels with a black neighbor,
- AXIS is the surface area of the white skeleton,
- NODE, ENDS are respectively the number of nodes and free ends of the white skeleton.

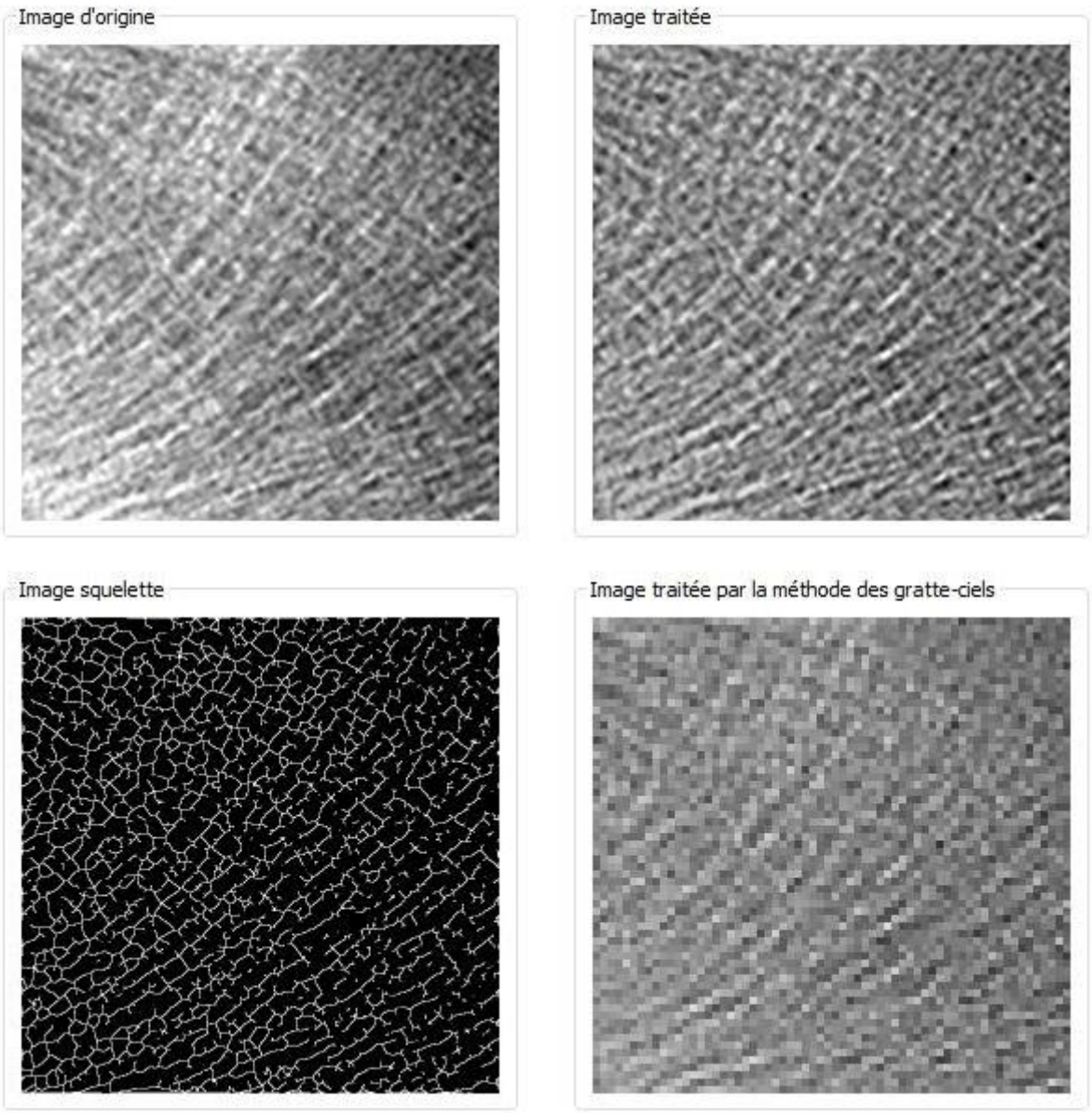

b) Run-lengths distribution:

The 256 grey level images are mapped to 16 grey levels to speed up computing time. Consecutive pixels of the same grey value in a given direction constitute a run [10, 11]. The run-length parameters are thus measured for the horizontal (H) and vertical (V) directions and the mean value is considered for analysis. The run length parameters have been extensively described elsewhere and comprise [10, 11]:

- SRE (HSRE and VSRE) - Short Run Emphasis is highly dependent on the occurrence of short runs and is expected large for fine textures.
- LRE (HLRE and VLRE) - Long Run Emphasis is highly dependent on the occurrence of long runs and is expected large for coarse structural textures.

- GLN (HGLN and VGLN) - Grey Level Non-uniformity measures the similarity of grey level values throughout the image. The GLN is expected small if the grey level values are alike throughout the image.
- RLN (HRLN and VRLN) - Run Length Non-uniformity measures the similarities of the length of the runs throughout the image. The RLN is expected small if the run lengths are alike throughout the image.
- RP (HRP and VRP) - Run Percentage measures the homogeneity and the distribution of runs of an image in a specific direction. RP is expected large for image with a homogenous texture.
- LGRE (HLGRE and VLGRE) - Low grey level run emphasis is dependent on the occurrence of runs with a low grey level (black, deep grey).
- HGRE (HHGRE and VHGRE) - High grey level run emphasis is dependent on the occurrence of runs with a high grey level (white, light grey).

c) The "skyscrapers" fractal analysis

A bitmap image *A* can also be considered as an x*y surface. Pixels which constitute the image can be viewed as skyscrapers whose height is represented by the grey level, the roof of the skyscrapers being a square of side ε [12]. The surface areas of the image $A(\varepsilon)$ is obtained by measuring the sum of the top surfaces (ε^2) and sum of the exposed lateral sides of the skyscrapers. The grey levels of adjacent pixels are then averaged in squares of ε: 2, 4, 8, 16 and 32 pixels to produce new images and $A(\varepsilon)$ is calculated for each ε. The fractal dimension (Kolmogorov) of the surface is determined by plotting a graph of log $A(\varepsilon)$ *vs.* log ε. The linear regression line is computed only on the aligned points by the least square method. The fractal dimension is obtained as $D_{SKY} = 2 - \text{slope}$.

d) The "blanket" fractal analysis

We have used the method described by Peleg et al., for calculating another fractal dimension by using dilatation and erosion of an image [13]. The structuring element used is a cross. Given a size ε for the structuring element, a dilatation and an erosion of the image provided two covering new images: respectively the upper u_ε and the lower b_ε. Then V_ε , the volume of the blanket, i.e., the volume enclosed between the dilatation and erosion images is measured and $A_{(\varepsilon)}$, the surface area measured with size ε is the mean of $(V_\varepsilon - V_{(\varepsilon-1)})$. The fractal dimension D_{BLANK} is

computed as above described by plotting log $A_{(\varepsilon)}$ against log (ε) and searching the slope coefficient by the least square method. A fractal dimension is obtained with each structuring element: $D_{BLANK}\oplus$ for the cross, D_{BLANK} — and $D_{BLANK}|$ for respectively the horizontal and vertical rods.

Recently, we published that the method provided reliable correlations between the vertebra and radius in a series of human cadavers with osteoporosis [14]. The method has also been applied to evaluate bone loss in the rat induced by Botox injection [3] or by metastatic cells [15]. Texture analysis parameters correlate with those obtained by histomorphometry [16] or microcomputed tomography [17] and medullary fat can influence the results (as with any X-ray analysis) [18].

However, please note that these most of these algorithms apply to 512 x 512 images. In other studies on the alveolar bone, it was not possible to use all of these methods and only the run length technique was available. Bone loss at the mandible was evidenced in the rat after orchidectomy [19]; healing of the maxillary sinus was studied on repetitive CT scans in patients having had a bone graft before placing bone implants [20]. On CT-images, the interest of the method depends of the thickness of the bone sections [7]. Other applications of texture analysis of images have been proposed to characterize the surface roughness of materials [21] and the swelling of hydrogels [22]. Texture analysis can also be applied on microscopic images. We have used these methods to analyze the chromatin compaction of the nucleus in thiazolidine treated pre-osteoblastic cells which differentiate into adipocytes [23]. The method was also applied to gray images of the microtubules of the cytoskeleton of osteoblasts [24].

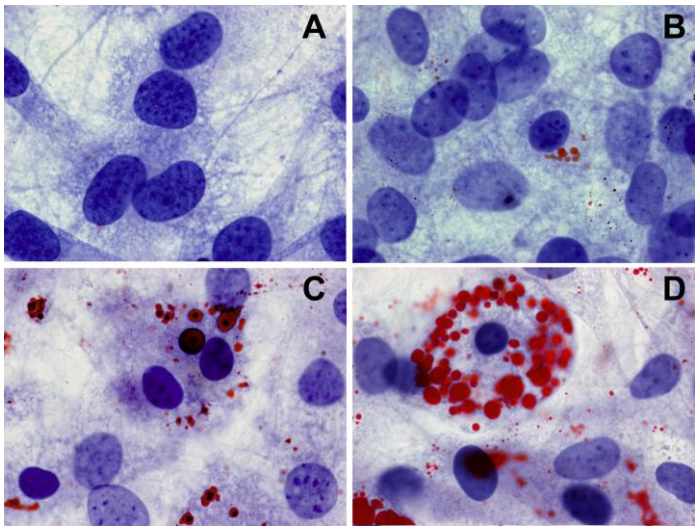

Note the compaction of chromatin as the cytoplasm accumulates lipid droplets

References

References preceded with ► are from our laboratory

[1] Buckland-Wright JC, Lynch JA, and Macfarlane DG. Fractal signature analysis measures cancellous bone organisation in macroradiographs of patients with knee osteoarthritis. Annals of Rheumatic Diseases 1996;55:749-55.

[2] Caldwell CB, Moran EL, and Bogoh ER. Fractal dimension as a measure of altered trabecular bone in experimental inflammatory arthritis. J Bone Miner Res 1998;13:978-85.

[3] ►Chappard D, Chennebault A, Moreau M, Legrand E, Audran M, and Baslé MF. Texture analysis of X-ray radiographs is a more reliable descriptor of bone loss than mineral content in a rat model of localized disuse induced by the Clostridium botulinum toxin. Bone 2001;28:72-9.

[4] Faulkner KG, and Pocock N. Future methods in the assessment of bone mass and structure. Best Pract Res Clin Rheumatol 2001;15:359-83.

[5] Geraets WG, Van der Stelt PF, Netelenbos CJ, and Elders PJ. A new method for automatic recognition of the radiographic trabecular pattern. J Bone Miner Res 1990;5:227-33.

[6] Haidekker MA, Andresen R, Evertsz CJG, Banzer D, and Peitgen HO. Assessing the degree of osteoporosis in the axial skeleton using the dependence of the fractal dimension on the grey level threshold. Brit J Radiol 1997;70:586-93.

[7] ►Guggenbuhl P, Chappard D, Garreau M, Bansard JY, Chales G, and Rolland Y. Reproducibility of CT-based bone texture parameters of cancellous calf bone samples: influence of slice thickness. Eur J Radiol 2008;67:514-20.

[8] ►Chappard D, Baslé MF, Legrand E, and Audran M. New laboratory tools in the assessment of bone quality. Osteoporos Int 2011;22:2225-40.

[9] Link TM, Majumdar S, Konermann W, Meier N, Lin JC, Newitt D, et al. Texture analysis of direct magnification radiographs of vertebral specimens: correlation with bone mineral density and biomechanical properties. Acad Radiol 1997;4:167-76.

[10] Galloway MM. Texture analysis using gray level run lengths. Comput Graph Image Proc 1975;4:172-79.

[11] Chu A, Sehgal CM, and Greenleaf JF. Use of gray value distribution of run lengths for texture analysis. Patt Recogn Lett 1990;11:415-19.

[12] Caldwell CB, Moran EL, and Bogoch ER. Fractal dimension as a measure of altered trabecular bone in experimental inflammatory arthritis. J Bone Miner Res 1998;13:978-85.

[13] Peleg S, Naor J, Hartley R, and Avnir D. Multiple resolution texture analysis and classification. IEEE Trans Pattern Anal Mach Intell 1984;6:518-23.

[14] ►Mallard F, Bouvard B, Mercier P, Bizot P, Cronier P, and Chappard D. Trabecular microarchitecture in established osteoporosis: Relationship between vertebrae, distal radius and calcaneus by X-ray imaging texture analysis. Orthop Traumatol Surg Res 2013;99:52-59.

[15] ►Blouin S, Moreau MF, Baslé MF, and Chappard D. Relations between radiograph texture analysis and microcomputed tomography in two rat models of bone metastases. Cells Tissues Organs 2006;182:182-92.

[16] ►Chappard D, Guggenbuhl P, Legrand E, Baslé MF, and Audran M. Texture analysis of X-ray radiographs is correlated with bone histomorphometry. J Bone Miner Metab 2005;23:24-9.

[17] ►Guggenbuhl P, Bodic F, Hamel L, Baslé MF, and Chappard D. Texture analysis of X-ray radiographs of iliac bone is correlated with bone micro-CT. Osteoporos Int 2006;17:447-54.

[18] ►Chappard D, Pascaretti-Grizon F, Gallois Y, Mercier P, Baslé MF, and Audran M. Medullar fat influences texture analysis of trabecular microarchitecture on X-ray radiographs. Eur J Radiol 2006;58:404-10.

[19] ►Lerouxel E, Libouban H, Moreau MF, Baslé MF, Audran M, and Chappard D. Mandibular bone loss in an animal model of male osteoporosis (orchidectomized rat): a radiographic and densitometric study. Osteoporos Int 2004;15:814-9.

[20] ►Marchand-Libouban H, Guillaume B, Bellaiche N, and Chappard D. Texture analysis of computed tomographic images in osteoporotic patients with sinus lift bone graft reconstruction. Clin Oral Investig 2012:DOI 10.1007/s00784-012-0808-z.

[21] ►Chappard D, Degasne I, Huré G, Legrand E, Audran M, and Baslé MF. Image analysis measurements of roughness by texture and fractal analysis correlate with contact profilometry. Biomaterials 2003;24:1399-407.

[22] ►Mabilleau G, Baslé MF, and Chappard D. Evaluation of surface roughness of hydrogels by fractal texture analysis during swelling. Langmuir 2006;22:4843-5.

[23] ►Chappard D, Marchand-Libouban H, Moreau MF, and Basle MF. Thiazolidinediones cause compaction of nuclear heterochromatin in the pluripotent mesenchymal cell line C3H10T1/2 when inducing an adipogenic phenotype. Anal Quant Cytol Histol 2013;35:85-94.

[24] ►Demais V, Audrain C, Mabilleau G, Chappard D, and Baslé MF. Diversity of bone matrix adhesion proteins modulates osteoblast attachment and organization of actin cytoskeleton. Morphologie 2014;98:53-64.